BRAC University Journal, vol. VI1, no. 1 & 2, 2010, pp. 9-14

X-RAY STUDIES AND MAGNETIC PROPERTIES OF *Ni-Cu-Zn* FERRITE

M. L. Rahman
Department of Mathematics and Natural Sciences
BRAC University, 66 Mohakhali, Dhaka-1212, Bangladesh
Email: lutfor_59@yahoo.com

and

S. T. Mahmud
Department of Physics
Bangladesh University of Engineering and Technology, Dhaka-1000, Bangladesh

and

A. K. M. Akther Hossain
Department of Physics
Bangladesh University of Engineering and Technology,Dhaka-1000, Bangladesh

ABSTRACT

The effect of Cu^{2+} on the physical and magnetic properties of *Ni-Zn* ferrite prepared by the auto combustion technique has been studied. From the X-ray diffraction patterns it is seen that the sample has a single phase cubic spinel structure. The bulk density, average grain size and initial permeability increase with increasing sintering temperature up to an optimum temperature. Beyond that temperature all these properties decrease.

Key words: Ferrites, x-ray diffraction, initial permeability, bond length, hopping length.

I. INTRODUCTION

Magnetic ferrites have been studied extensively due to their wide field of technological applications in telecommunication and electronic industry. Among the soft magnetic ferrites, Ni-Cu-Zn ferrites are commercially important due to their application in different devices such as transformer cores, high quality filters, read-write heads for high speed digital tape and operating devices [1]. Such a large number of potential applications of Ni-Cu-Zn ferrite are possible due to their high resistivity, low dielectric loss, high Curie temperature, high permeability; etc [2].The crystal structure of these materials controls their physical properties. The structural as well as magnetic properties of spinel ferrites are dependent on several factors such as preparation method, sintering process [3] and constituent elements. According to their crystal structure, spinel-type ferrites have natural superlattice. They have tetrahedral A sites and octahedral B sites in AB_2O_4 crystal structure. Various cations can be placed at the A sites and B sites to tune their magnetic properties. Depending on the A site and B site cations, ferromagnetic, antiferromagnetic, spin-glass and paramagnetic behavior are observed in these spinel ferrites [4-7]. Owing to impact of fine particles on properties of Ni-Cu-Zn ferrites and considering its possible consequent effects on the technological applications, it has been decided to study the structural and magnetic properties of Ni-Cu-Zn ferrites prepared by combustion technique.

II. EXPERIMENTAL

The sample of $Ni_{0.20}Cu_{0.30}Zn_{0.50}Fe_2O_4$ has been prepared through auto combustion method. The stoichiometric amounts of highly pure powders of $Ni(NO_3)_2.3H_2O$, $Cu(NO_3)_2.3H_2O$, $Zn(NO_3)_2.6H_2O$, $Fe(NO_3)_3.9H_2O$ have been dissolved in ethanol. Then the solution has been heated at 70°C to transform into gel, the dried gel has burnt out to form a fluffy loose powder. Then the resultant powder has been calcined at 850°C for five hours and then pressed uniaxially into disk shaped (about 10 mm outer diameter, 2-3 mm thickness) and toroid shaped (about 10 mm outer diameter, 5 mm

inner diameter, and 3 mm thickness) samples. The samples have been sintered at 1200°C, 1250°C and 1300°C for five hours in air, the temperature ramps were 10°C/min for heating and 5°C/min for cooling respectively. The physical or bulk densities ρ_E of the samples have been determined with water medium using the expression $\rho_B = (W\rho/W - W')g/cm^3$, where W and W' are the weight of the sample in air and water, respectively and ρ is the density of water at room temperature [8]. The theoretical density ρ_{th} has been calculated using the expression: $\rho_{th} = (8M/N_A a_o^3)g/cm^3$, where N_A is Avogadro's number, M is the molecular weight of the sample. The porosity has been calculated from the relation $\{100(\rho_{th} - \rho_B)/\rho_{th}\}\%$, where ρ_B is the measured bulk density. Average grain sizes (grain diameter) of the sample have been determined from optical micrographs by linear intercept technique [9].The frequency characteristics of $Ni_{0.20}Cu_{0.30}Zn_{0.50}Fe_2O_4$ ferrite sample i.e. the initial permeability spectra have been investigated using a Wayne Kerr precision impedance analyzer (Model no. 6520A). The complex permeability measurements on toroid shaped specimens have been carried out at room temperature of the sample in the frequency range 1 kHz-15MHz. The values of the measured parameters obtained as a function of frequency and the real part (μ') of the complex permeability have been calculated using the following relations $\mu' = L_s/L_o$, where L_s is the self inductance of the sample core and $L_o = (\mu_o N^2 h/2\pi) \ln(r_o/r_i)$ is derived geometrically. L_o is the inductance of the winding coil without the sample core, N is the number of turns of the coil (N = 5), h is the thickness, r_o is the outer radius and r_i is the inner radius of the toroidal specimen. The relative quality factor has been calculated from the relation: $Q = \mu'/\tan\delta$, where $\tan\delta$ is the loss factor.

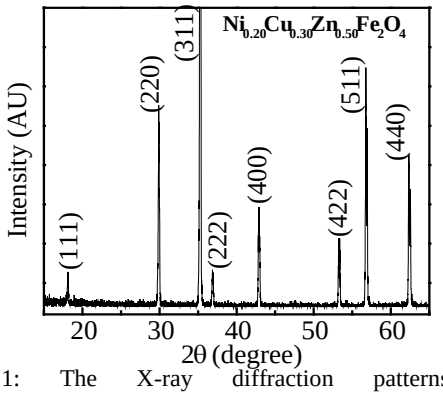

Fig.1: The X-ray diffraction patterns for $Ni_{0.20}Cu_{0.30}Zn_{0.50}Fe_2O_4$

III. RESULTS AND DISCUSSION

A. X-ray diffraction analysis

The x-ray diffraction (XRD) pattern (Fig.1) shows that the sample has single-cubic spinel structure. Analyzing the XRD patterns it is observed that the positions of the peaks agree with the earlier reported values [10]. The *d*-spacing for each peak is recorded automatically and then the lattice parameter (a) is calculated from the relation $a = d_{hkl}(h^2 + k^2 + l^2)^{1/2}$ .The values of lattice parameter '*a*' of all the peaks for the sample obtained for each reflected plane are plotted against the Nelson-Riley function, $F(\theta)$, (Fig.2) where $F(\theta) = (1/2)[(\cos^2\theta/\sin\theta) + (\cos^2\theta/\theta)]$;θ is the Bragg's angle. A Straight line fit has been obtained and the accurate value or the true lattice parameter a_o has been determined from the extrapolation of these lines to $F(\theta) = 0$ [11].The true value of the lattice constant a_o is 8.4062 Å; where as the average and theoretical values are 8.3489 Å and 8.1148 Å respectively. The theoretical values of a_{th} is little smaller than the values of *a* and a_o.The theoretic-

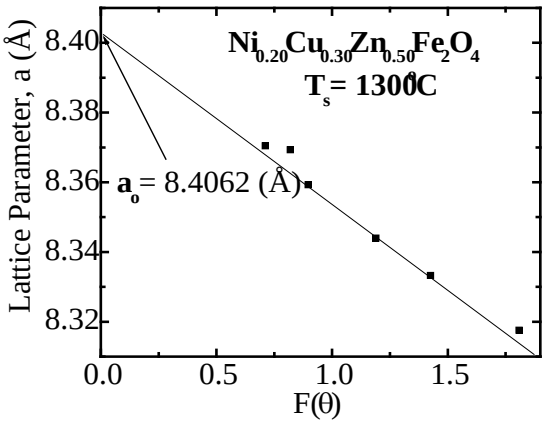

Fig. 2: The Nelson- Riley function F(θ) vs lattice parameter for $Ni_{0.20}Cu_{0.30}Zn_{0.50}Fe_2O_4$ sintered at 1300^0C in air for 5hr

cal lattice parameter a_{th} calculated from the relation [12] $a_{th} = (8/3\sqrt{3})[r_A + R_O] + \sqrt{3}[r_B + R_O]$ where r_A and r_B the mean ionic radius of the A-sites (r_A) and B-sites (r_B) which were estimated cation distribution $(Zn_{0.50}Fe_{0.50})[Ni_{0.20}Cu_{0.30}Fe_{1.50}]O_4$ is supported by X-ray studies and R_O is the radius of oxygen ion which is 1.46 Å [13]. Using the value of *a*, the radius of oxygen ion R_O and r_A in the following expression, the value of the oxygen positional parameter *u* can be calculated [13]

$r_A = (u - 1/4)a\sqrt{3} - R_O$. The calculated value of *u* is 0.397 Å. Substituting the value of *a* and *u* into the following expression the tetrahedral and octahedral bond length (*A-O* and *B-O*) can be calculated as follows [13]

$A - O = a\sqrt{3}(u - 1/4)$ and

$B - O = a\left[3u^2 - (11/4)u + 43/64\right]^{1/2}$

Table 1**:** The density, porosity, average grain size, natural resonance frequency, real part of initial permeability, and Q_{max} for $Ni_{0.20}Cu_{0.30}Zn_{0.50}Fe_2O_4$ sintered at various temperatures, T_s, with fixed dwell time 5 h.

x	T_s (^0C)	ρ_{th} (g/cm^3)	ρ_B (g/cm^3)	*P (%)*	Grain Size (μm)	f_r (kHz)	μ_i' (at 100 kHz)	Q_{max}
	1200		4.14	22.63	34	62	570	1208
0.30	1250	5.35	4.29	19.82	37	33	576	1689
	1300		4.18	21.88	28	96	398	2131

The calculated values of *A-O* and *B-O* are 2.1403 Å and 1.9343 Å respectively. The hopping length *L* between magnetic ions (the distance between the ions) in the tetrahedral A-sites is given by $L_A = a\sqrt{3}/4$ and in the octahedral B-sites by $L_B = a\sqrt{2}/4$ [13].The values of the hopping length L_A and L_B are found to be 3.6399 Å and 2.9720 Å. The measured theoretical density, bulk density and porosity for the sample sintered at different temperatures are given in Table-1. Figure 3 shows the density and porosity as a function of sintering temperature, T_s. The density of the $Ni_{0.20}Cu_{0.30}Zn_{0.50}Fe_2O_4$ samples increases as the sintering temperature increases from 1200°C to 1250°C and above 1250°C the density decreases. On the other hand, porosity (*P)* of the sample decreases as increasing sintering temperature up to 1250°C, and above 1250°C the porosity increases. The increase in density with sintering temperature is expected. This is because during the sintering process, the thermal energy generates a force that drives the grain boundaries to grow over pores, thereby decreasing the pore volume and denser the material. At higher sintering temperatures the density decreases because the intragranular porosity increases resulting from discontinuous grain growth. The discontinuous growth of grain rises with temperature and hence, contributing toward the reduction of the bulk density. This result agrees with that previously reported in case of *MgCuZn* ferrites [14].

B. Microstructures of $Ni_{0.20}Cu_{0.30}Zn_{0.50}Fe_2O_4$

The optical micrographs of $Ni_{0.20}Cu_{0.30}Zn_{0.50}Fe_2O_4$ sintered at different temperature are shown in Fig. 4. It can be seen from Table 1 that the average grain size of the samples increases with the increase of sintering temperature up to 1250°C. Beyond this temperature grain size decreases. The grain size has an important influence on the domain wall contribution in the magnetization process. When the grain growth rate is very high, pores may be left behind by rapidly moving grain boundaries, resulting in pores that are trapped inside the grains. This intragranular porosity is practically impossible to eliminate, leading to poor magnetic and mechanical properties.

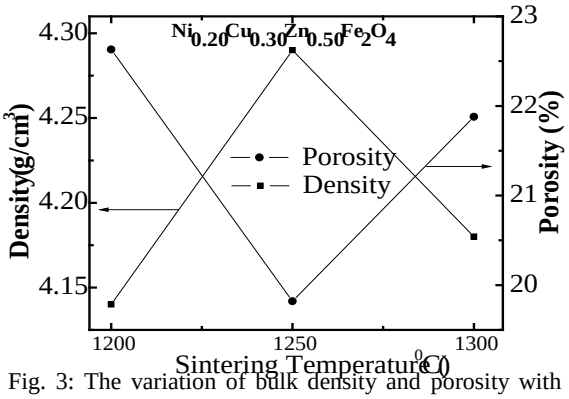

Fig. 3: The variation of bulk density and porosity with sintering temperature for $Ni_{0.20}Cu_{0.30}Zn_{0.50}Fe_2O_4$

C. Initial permeability

Fig. 5 shows the initial permeability spectra for $Ni_{0.20}Cu_{0.30}Zn_{0.50}Fe_2O_4$ samples sintered at different sintering temperatures. It is observed that the real part of initial permeability, μ_i',of $Ni_{0.20}Cu_{0.30}Zn_{0.50}Fe_2O_4$ ferrite increases from 570 to 576 as sintering temperature, T_s increases from 1200°C to 1250°C and then decreases. The values of μ_i' at 100 kHz are tabulated in Table 1. It is well known that the permeability of polycrystalline ferrite is

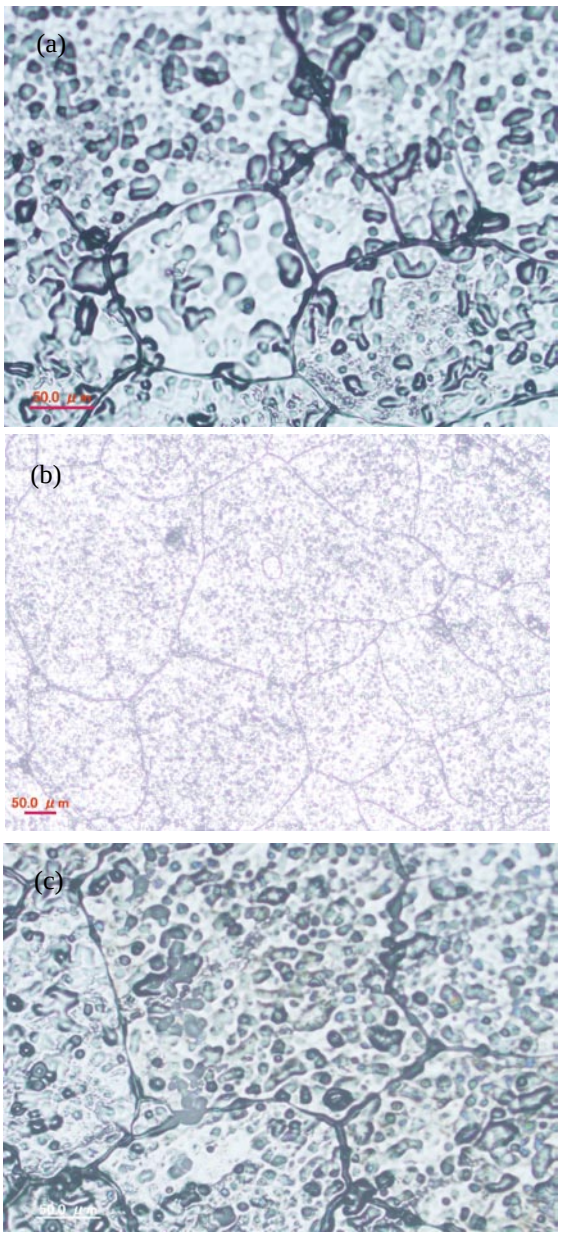

Fig. 4: The microstructure of $Ni_{0.20}Cu_{0.30}Zn_{0.50}Fe_2O_4$ samples sintered at (a) 1200°C (b) 1250°C and (c)1300°C

related to two different magnetizing mechanisms: spin rotation and domain wall motion [15, 16], which can be described as follows:

$$\mu_i = 1 + \chi_w + \chi_{spin}$$

where χ_w is the domain wall susceptibility; χ_{spin} is intrinsic rotational susceptibility. χ_w and χ_{spin} may be written as $: \chi_w = 3\pi M_s^2 D / 4\gamma$ and $\chi_{spin} = 2\pi M_s^2 / K$ with M_s is the saturation magnetization, K is the total anisotropy, D is the average grain diameter, and γ the domain wall energy. Thus the domain wall motion is affected by the grain size and enhanced with the increase of grain size. The initial permeability is, therefore, a function of grain size. In the present microstructural study it is seen that with the increasing sintering temperature, grain sizes increase first and then decrease at higher sintering temperature. Larger grains tend to consist of a greater number of domain walls. The magnetization caused by domain wall movement requires less energy than that required by domain rotation. As the number of walls increases with the grain sizes, the contribution of wall movement to magnetization increases. Therefore, permeability increases with the increase of sintering temperature. However, it is observed that μ_i' is maximum at optimum T_s (depending on sample composition) as shown in Fig. 6. If the sintering temperature is higherthan that of the optimum T_s, μ_i' decreases. It is possible that the samples sintered at higher sintering temperatures (> optimum T_s) may increase the number of pores within the grains which results in a decrease in permeability by pinning domain walls. Similar behaviour was observed by Guillaud in *Mn-Zn* ferrites [17].

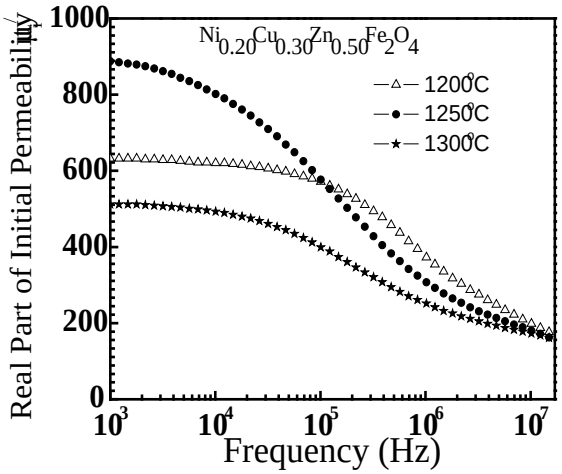

Fig. 5: The frequency dependence of μ_i' for $Ni_{0.20}Cu_{0.30}Zn_{0.50}Fe_2O_4$ samples sintered at different T_s

It is also observed that the higher the permeability of the materials, the lower the frequency of the onset of ferro magnetic resonance. This really confirms with Snoek's limit $f_r \mu_i' =$ constant [18], where f_r is the resonance frequency for the domain

wall motion, above which μ_i' decreases. It is seen that the resonance frequency decreases with increase in sintering temperature. As sintering temperature increases, the domain wall relaxation frequency shifted from 62 to 33 kHz but at higher sintering temperature i.e. 1300°C it increases again to 96 kHz. The relaxation frequency, f_r, for all samples is listed in Table 1. The variation of relative quality factors, Q with frequency for $Ni_{0.20}Cu_{0.30}Zn_{0.50}Fe_2O_4$ sintered at various temperatures is shown in Fig.7. The maximum Q value is about 2131 which occurs at T_s=1300°C. At higher frequencies, Q value decreases rapidly. It is also observed that Q increase with the increase in sintering temperature.

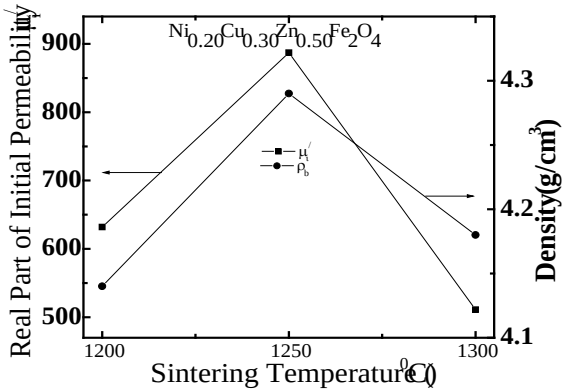

Fig.6: The variation of μ_i' and ρ_B with T_s for $Ni_{0.20}Cu_{0.30}Zn_{0.50}Fe_2O_4$

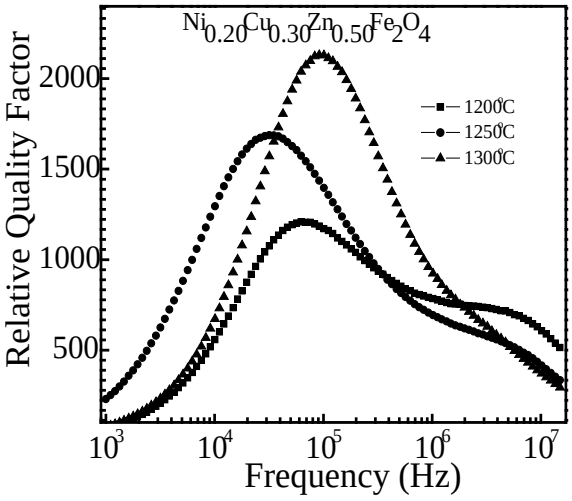

Fig.7**:** The variation of relative quality factor, Q, with frequency for $Ni_{0.20}Cu_{0.30}Zn_{0.50}Fe_2O_4$ sintered at different temperature

V. CONCLUSIONS

The theoretical value of the lattice constant is smaller than the true and average lattice constant. The bulk density, grain size and initial permeability of ferrite $Ni_{0.20}Cu_{0.30}Zn_{0.50}Fe_2O_4$ increases with increasing sintering temperature up to an optimum sintering temperature, T_s and beyond that optimum temperature all those properties decreases. With the increasing sintering temperature the relaxation frequency decreases first and then increases where as the relative quality factor increases. The polycrystalline $Ni_{0.20}Cu_{0.30}Zn_{0.50}Fe_2O_4$ ferrite sintered at 1300°C shows the highest relative quality factor.

Acknowledgements

The present study was supported by Bangladesh University of Engineering & Technology (BUET). One of the authors M. L. Rahman wishes to thank the Department of Mathematics and Natural Sciences of BRAC University for providing the facilities. Author also would like to express his gratitude to Professor A. A. Z. Ahmad for a critical reading of the manuscript and for making helpful suggestions.

REFERENCES

[1] G. X. Xi, L. Yang, M. Lu: "Study on preparation of nanocrystalline ferrites using spent alkaline Zn–Mn batteries" *Mater. Lett*., **60,** pp 3582-3585. (2006).

[2] A. Verma, T. C. Goel, R. G. Mendirath: "High-resistivity nickel–zinc ferrites by the citrate precursor method" *J. Magn. Magn. Mater*., **192,** pp 271-276. (1999).

[3] P. Yadoji, R. Peelamedu, D. Agrawal, R.Roy: "Microwave sintering of Ni–Zn ferrites: comparison with conventional sintering" *Mater. Sci. Eng. B.*, **98,** pp 269-278. (2003).

[4] N.S. Satya Murthy,M.G. Natera,S.i. Youssef, R.J. Begum, C.M. Srivastava: "Yafet-Kittel Angles in Zinc-Nickel Ferrites" *Phys. Rev.*, **181(2),** pp 969-977. (1969).

[5] V. C. Wilson, J. S. Kasper: "Neutron Diffraction Studies of a Nickel Zinc Ferrite" *Phys. Rev*., **95(6),** pp 1408-1411. (1954).

[6] L.K. Leung, B.J. Evans, A.H. Morish: "Low-Temperature Mössbauer Study of a Nickel-Zinc Ferrite: $Zn_xNi_{1-x}Fe_2O_4$" *Phys. Rev. B,* **8(1),** pp 29-43. (1973).

[7] J.M. Daniels, A. Rosenewaig: "Mössbauer study of the Ni–Zn ferrite system" *Can. J. Phys*., **48(4),** pp 381-396. (1970).

[8] A.B. Gadkari,T.J. Shinde, P.N. Vasambekar: "Structural and magnetic properties of nanocrystalline Mg-Cd ferrites prepared by oxalate co-precipitation method" *J. Mater Sci: Mater Electron,* **21(1)**, pp 96-103. (2010).

[9] A. K. M. Akther Hossain: *Investigation of colossal magnetoresistance in bulk and thick film magnetites*, Ph. D. Thesis, Imperial College, London. (1998).

[10] C. Rath, S. Anand, R. P. Das, K. K. Sahu, S. D. Kulkarni, S. K. Date and N. C. Mishra: "Dependence on Cation Distribution of Particle Size, Lattice Parameter, and Magnetic Properties in Nanosize Mn–Zn Ferrite" *J. Appl. Phys.*, **91(4)**, pp 2211-215. (2002).

[11] B.D. Cullity: *Elements of X-ray Diffraction*, Second printing, Addison-Wesley Publishing Company, Inc, USA. (1959).

[12] A.A. Yousef,M.E. Elzain, S.A. Mazen, H.H. Sutherland, M.A. Abdallah, S.F. Mansour: "A Mossbauer and X-ray diffraction investigation of Li-Ti ferrites " *J. Phys. Condens. Matter*., **6(29)**, pp 5717-5724. (1994).

[13] M.A. Amer,M. El Hiti: "Mössbauer and X-ray studies for $Ni_{0.2}Zn_xMg_{0.8-x}Fe_2O_4$ ferrites" *J. Magn. Magn. Mater.*, **234**, pp 118-125. (2001).

[14] S.R. Murthy: "Low temperature sintering of MgCuZn ferrite and its electrical and magnetic properties" *Bull. Mater. Sci.*, **24(4)**, pp 379-383. (2001).

[15] Y. Mi, H. Jun: "Preparation of high-permeability NiCuZn ferrite" *J. Zhejiang Uni. Sci.*, **6B**(6), pp 580-583. (2005).

[16] T. Tsutaoka, M. Ueshima, T. Tokunaga, T. Nakamura and K. Hatakeyama: "Frequency dispersion and temperature variation of complex permeability of Ni–Zn ferrite composite materials" *J. Appl. Phys.*, **78(6)**, pp 3983-3991. (1995).

[17] C. Guillaud: "The properties of manganese-zinc ferrites and the physical processes governing them", *Proceedings* of the *IEE*, **104B**, pp 165–178. *(*1957*)*.

[18] J. L. Snoek: "Dispersion and absorption in magnetic ferrites at frequencies above one Mc/s" *Physica*, **14(4)**, pp 207-217. (1948).